Chem Biol Drug Des 2013; **81:** 185–197

Research Article

Molecular Modeling of a Phenyl-Amidine Class of NMDA Receptor Antagonists and the Rational Design of New Triazolyl-Amidine Derivatives

Paula A. Abreu[1,2,*], Helena C. Castro[1], Roberto Paes-de-Carvalho[3], Carlos R. Rodrigues[4], Viveca Giongo[1,5], Izabel C. N. P. Paixão[5], Marcos V. Santana[1], Jainne M. Ferreira[3], Octavia M. Caversan[3], Raquel A. C. Leão[6], Luana M. S. Marins[6], André M. Henriques[6], Florence M. C. Farias[6], Magaly G. Albuquerque[7] and Sergio Pinheiro[6,*]

[1]LABiEMol, Departamento de Biologia Celular e Molecular, Instituto de Biologia, Outeiro de São João Baptista, Campus Valonguinho, Centro CEP 24210-130 Universidade Federal Fluminense (UFF), Niterói, RJ, Brazil
[2]LaMCiFar, Universidade Federal do Rio de Janeiro UFRJ-Campus Macaé, Av. São José do Barreto, Macaé CEP 27965-045 RJ, Brazil
[3]Laboratório de Neurobiologia Celular, Instituto de Biologia, UFF, Outeiro de São João Baptista, Campus Valonguinho. CEP 24020-150 Niterói, RJ, Brazil
[4]ModMolQSAR, Faculdade de Farmácia, UFRJ, Av Carlos Chagas Filho, 373 Cidade Universitária, CEP 21941-599 Rio de Janeiro, RJ, Brazil
[5]Laboratório de Virologia Molecular, Instituto de Biologia, UFF, Outeiro de São João Baptista, Campus Valonguinho. CEP 24020-150 Niterói, RJ, Brazil
[6]Laboratório de Síntese Assimétrica, Instituto de Química, UFF, Outeiro de São João Baptista, Campus Valonguinho. CEP 24020-150 Niterói, RJ, Brazil
[7]LabMMol, Instituto de Química, UFRJ, Cidade Universitária, Ilha do Fundao CEP 21949-900 Rio de Janeiro, RJ, Brazil
**Corresponding authors: Paula A. Abreu, abreu_pa@yahoo.com.br; Sergio Pinheiro, spinuff@gmail.com*

Recently, many efforts have been made to develop *N*-methyl-D-aspartic acid receptor antagonists for treating different pathological conditions such as thrombo-embolic stroke, traumatic head injury, Huntington's, Parkinson's, and Alzheimer's diseases). However, as side-effects limit the use of most antagonists, new drugs are still required. In this work, we performed a (quantitative) structure-activity relationship analysis of 17 phenyl-amidine derivatives (1a–1q), reported as *N*-methyl-D-aspartic acid receptor antagonists, and used this data to rationally design the triazolyl-amidines. The best (quantitative) structure-activity relationship model constructed by multiple linear regression analysis presented high data fitting (R = 0.914) was able to explain 83.6% of the biological data variance (R^2 = 0.836), presented a satisfactory internal predictive ability (Q^2 = 0.609) and contained the descriptors (E_{HOMO}, Ovality and cLogP). Our assays confirmed that glutamate promotes an extensive cell death in avian neurons (77%) and 2a and 2b protected the neurons from the glutamate effect (from 77% to 27% and 45%, respectively). The results of neurotoxicity and cytotoxicity on Vero cells suggested the favorable profile of 2a and 2b. Also, the molecular modeling used to predict the activity, the interaction with the receptor and the pharmacokinetic and toxicity of the triazolyl-amidines pointed them as a promising class for further exploration as *N*-methyl-D-aspartic acid receptor antagonists.

Key words: drug design, molecular modeling, NMDA receptor antagonists, phenyl-amidine, triazolyl-amidine

Received 29 January 2012, revised 6 August 2012 and accepted for publication 13 September 2012

The *N*-methyl-D-aspartic acid (NMDA) receptors are a group of ionotropic glutamate receptors that plays an important role in different physiological functions, including the neuronal development, synaptic plasticity, learning, and memory (1). NMDA receptor is composed of multiple protein subunits, GLUN1, GLUN2 (A–D), and GLUN3 (A–B) in different combinations. In general, the physiological receptor is a heteromer, containing GLUN1 subunit with one or two GLUN2 subunits, but different compositions may occur (2–4). Therefore, depending on the receptor composition both the electrophysiological and pharmacological properties may vary (4).

Due to its role, the over-stimulation of NMDA receptor has been implicated in several pathological conditions, involving neuronal death and degeneration (e.g., thrombo-embolic stroke, traumatic head injury, Parkinson's, Huntington's, and Alzheimer's diseases). Therefore, this pathological role has driven the search for NMDA receptor antagonists as a promising therapy (5–8). Currently, the use of NMDA receptor antagonists for acute and chronic neuronal diseases

 doi: 10.1111/cbdd.12056

therapy still present undesirable side-effects, such as motor deficit and sedation that limit their use (9–11). Importantly, the absence of GLUN2B message in the cerebellum suggests that a GLUN2B selective antagonist might not adversely affect the locomotor function (4,12–14).

Ifenprodil is a selective GLUN1/GLUN2B NMDA receptor antagonist that presents a safer side-effect profile than other non-selective antagonists (e.g., MK801). However, it still presents some side-effects similar to other NMDA receptor antagonists (e.g., Co101676, PD174494, and CI1041) (4,6) (Figure 1). Currently, many efforts are in progress to develop less toxic compounds for several neuropathological conditions, such as those based on styrylamidines (**I**), arylamidines (**II**), and cyclic benzamidines (**III**), that were described as orally efficacious selective GLUN1/GLUN2B NMDA receptor antagonists (Figure 1) (4,9,13,15–20).

Claiborne and co-workers (9) synthesized and reported the binding affinity data (i.e., Ki) for a series of 25 phenyl-amidines and for 17 of these compounds, they also reported the functional activity data (i.e., IC_{50}) as GLUN1/GLUN2B NMDA receptor antagonists with >100-fold selectivity for GLUN1/GLUN2B than for GLUN1/GLUN2A. Also, many compounds based on 1,2,3- and 1,2,4-triazoles have been described in the literature with important biological activities (21–23), such as antiplatelet (24), anticonvulsant (25), and anti-inflammatory profiles (26). Therefore, the aim of this work is to design and synthesize a new class of triazolyl-amidines, potential NMDA receptor antagonists, and evaluate their neuroprotective effects through glutamate-induced cellular death.

Methods and Materials

Quantitative structure-activity relationship studies and design of new triazolyl-amidines

The structure-activity relationship (SAR) and the quantitative structure-activity relationship (QSAR) studies were performed using as activity data the pIC_{50} (*M*) values of 17 compounds (*N* = 17) from the original data set (9). The 3D structure of a hypothetical non-substituted ($R_1 = R_2 = H$) derivative was submitted to the default systematic conformational analysis, available in the SPARTAN'08 software (Wavefunction Inc. Irvine, CA, USA), using the MMFF94 force field, and the most stable conformer was used to assemble the 3D structures of the 17 phenyl-amidines.

All structures were submitted to a full geometry optimization process, using the Austin Model 1 (AM1) semi-empirical Hamiltonian, and, subsequently, to a single-point energy *ab initio* calculation, at the 3-21G* level, both methods available in SPARTAN'08.

Molecular electrostatic potential (MEP) isoenergy surface maps were generated in the range from −25.0 (deepest red color) to +30.0 (deepest blue color) kcal/mol and superimposed onto a molecular surface of constant electron density of 0.002 e/au^3. Each point of the three dimensional molecular surface map expresses the electrostatic interaction energy value evaluated with a probe atom of positive unitary charge, providing an indication of the overall molecular size and location of attractive (negative) or repulsive (positive) electrostatic potentials shown in red and blue, respectively.

To perform the SAR/QSAR studies, descriptors from three general characteristics were calculated, that are, electronic, steric, and pharmacokinetic, which could be related to the biological response. The electronic descriptors correspond to frontier orbitals and molecular dipole moment (μ). The steric descriptors calculated with SPARTAN'08 correspond to molecular volume (MV), molecular surface area (MSA), and ovality (a ratio of volume and area, measuring the overall shape), while the pharmacokinetic descriptors, calculated with the Osiris Property Explorer (27) online system (http://www.organicchemistry.org/prog/peo/), correspond to the molecular mass (MM), the octanol/water partition coefficient (cLogP), water solubility (cLogS), and the number of hydrogen bond acceptors (HBA) and donors (HBD).

In QSAR, it is usual to split the data set in training set and test set, then, the training set is used to generate the QSAR model, and the test set is used for the external validation of the generated QSAR model. So, we have applied an internal validation procedure, named leave-one-out cross-validation (LOO-CV), using a combined genetic function approximation (GFA) algorithm and partial least-squares (PLS) regression approach, available in the WOLF v.6.2 software, and implemented with the Friedman's lack-of-fit (LOF) score, which prevent the models overfitting, Because it penalizes additional terms when identical least-square-error (LSE) values are observed. The equations (models) are compared according to the statistical parameters: *N* = number of terms (descriptors, independent variables); *R* = correlation coefficient; R^2 = quadratic correlation coefficient; *Q* = *R* after leave-one-out cross-validation; and $Q^2 = R^2$ after leave-one-out cross-validation. We also applied an external validation using three amidines described by Nguyen and co-workers (20) as the test set.

The same methodology was applied for both phenyl-amidines and the designed triazolyl-amidines. The design of the new class of triazolyl-amidines was based on strategies of molecular modification currently used in medicinal chemistry as bioisoterism, QSAR analysis and the maintenance of the pharmacophoric groups.

Chemistry

General: Flash chromatography was performed in 230–400 mesh silica gel (Merck). Melting points were determined on a Fischer-Johns apparatus, and 1H and 13C-NMR spectra were recorded in a Varian Unity Plus (300 MHz).

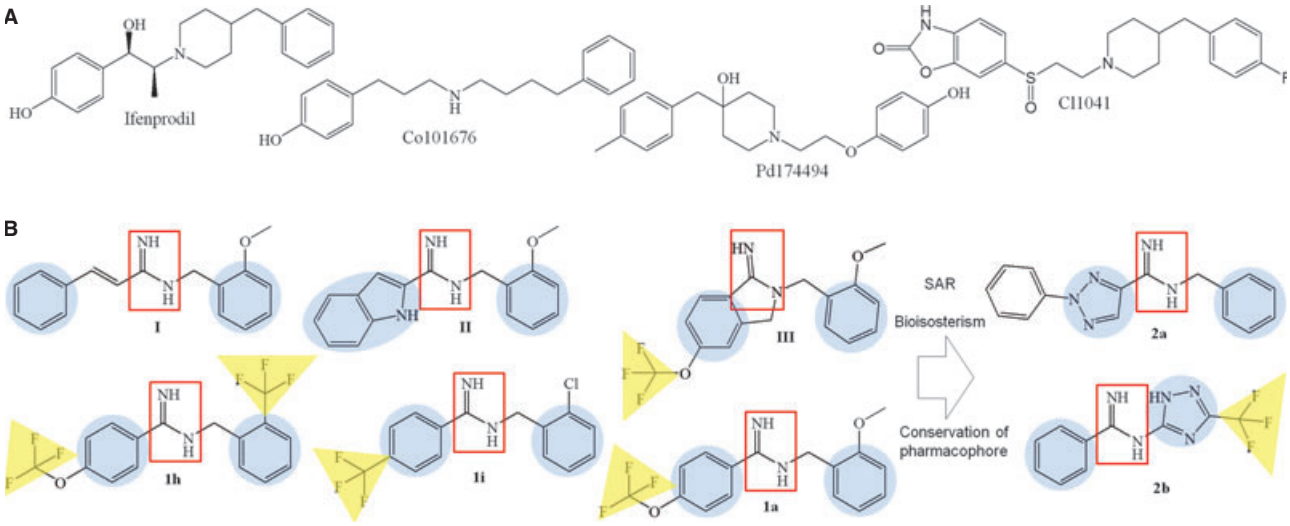

Figure 1: NMDA receptor antagonists described in the literature and rational design of new triazolyl-amidines (**2a**–**2b**).

N-Benzyl-2-phenyl-2H-(1,2,3)triazole-4-carboxamidine (**2a**): A DMSO (1 mL) solution of benzylamine (107 mg; 1 mmol) was added to a DMSO (2 mL) solution of **5** (213 mg; 1.25 mmol) and CuCl (124 mg; 1.25 mmol). The mixture was stirred under a nitrogen atmosphere, at 80 °C for 20 h. AcOEt (2 mL) and 50% aqueous NaOH (4 mL) were added. The mixture was vigorously stirred for 30 min. The filtered and the solid were washed with AcOEt (10 mL). The organic layer was dried over Na_2SO_4, and the volatiles were removed in vacuum. The residue was purified by flash chromatography on silica gel (10% AcOEt in hexane as the eluent) to give **2a** as a white solid (202 mg, 73% yield). Mp = 121–123 °C. IR (KBr, cm^{-1}): 3280, 3033, 2919, 1658, 1595, 1553, 1497, 1455, 1322, 1227, 1153, 970, 756, 697, 667; 1H-NMR (300 MHz, DMSO-*d*6, δ) 9.33 (m, 1H), 8.58 (s, 1H), 8.38 (ddd, J = 7.5 Hz, J = 3.2 Hz, J = 1.2 Hz, 2H), 7.73 (ddd, J = 8.7 Hz, J = 7.5 Hz, J = 1.7 Hz, 2H), 7.60 (tt, J = 8.7 Hz, J = 1.2 Hz, 1H), 7.50–7.45 (m, 4H), 7.40–7.34 (m, 1H), 4.63 (d, J = 6.3 Hz, 2H); 13C-NMR (75 MHz, DMSO-*d*6, δ) 159.2 (s), 144.2 (s), 139.2 (s), 138.9 (s), 136.4 (s), 129.8 (s), 128.6 (s), 128.4 (s), 127.4 (s), 126.9 (s), 118.9 (s), 42.2 (s).

N-(5-Trifluoromethyl-2H-(1,2,4)triazol-3-ylmethyl)-benzamidine (**2b**): A suspension of **6** (152 mg; 1 mmol) in benzonitrile (1 mL) was added to a benzonitrile (2 mL) solution of CuCl (124 mg; 1.25 mmol). The mixture was stirred, under a nitrogen atmosphere, at 80 °C for 20 h. AcOEt (2 mL) and 50% NaOH (4 mL) were added. The mixture was vigorously stirred for 30 min. The organic layer was washed consecutively with 3 M NH_4OH [until negative test for Cu (II) using 0.1 M $K_4Fe(CN)_6$], with 5% NH_4Cl (until neutralization), and then with water (15 mL). Subsequently, it was dried over Na_2SO_4, and the volatiles were removed in vacuum. The residue was crystallized from ethyl alcohol to give **2b** as a yellow solid (191 mg, 75% yield). Mp = 151 °C. IR (KBr, cm^{-1}): 3346, 3203, 3061, 2920, 2851, 1645, 1578, 1530, 1510, 1466, 1447, 1216, 1181, 1145, 1034, 1008, 860, 771, 743, 697 cm^{-1}; 1H-NMR (300 MHz, DMSO-*d*6, δ) 9.07 (s, 1H), 8.90 (s, 1H), 8.22 (s, 1H), 8.17–8.13 (m, 3H), 7.70–7.64 (m, 2H); 13CNMR (75 MHz, DMSO-*d*6, δ) 160.7 (s), 160.4 (s), 149.7 (q, J = 37 Hz), 134.6 (s), 131.8 (s), 128.7 (s), 127.7 (s), 119.8 (q, J = 269 Hz).

Biological activity assays

Neuroprotection from glutamate excitotoxicity

An earlier work showed that incubation of avian retinal neurons cultures with glutamate (1 mM) for 8 h promoted an intense cell death (28) that could be prevented by previous culture treatment with 10 μM ifenprodil (29). Thus, triazolyl-amidines **2a** and **2b** were tested for their neuroprotective potential profile by pre-incubating the purified cultures of avian retinal neurons, prepared as described elsewhere (28), with 100 nM of the compounds solubilized in dimethyl sulfoxide (DMSO) for 48 h in the same culture medium. Then, we added glutamate (1 mM) to the medium and after 8 h, the cultures were fixed and the number of viable cells was determined by counting at least five fields of 0.114 mm^2 of each dish using a phase contrast inverted microscope. **2a** and **2b** (100 nM) were also tested without the addition of glutamate to observe their effect on the avian culture. All experiments were made in triplicate at least three times.

Cytotoxicity assay

Monolayers of 104 Vero cells (African green monkey kidney) in 96-multiwell plates were treated with several concentrations (50, 250, 500, and 1000 μM) of triazolyl-amidines **2a** and **2b** for 72 h. The medium used was Dulbecco's Modified Eagle Medium (DMEM) with 5% of serum fetal bovine. Then, 50 μL of 3-(4,5-dimethylthiazol-2-yl)-2,5-diphenyltetrazolium bromide (MTT, Sigma) solution (1 mg/mL of

MTT in solvent) was added to evaluate cell viability according to procedures described elsewhere (31). The 50% cytotoxic concentration (CC_{50}) was calculated by linear regression analysis of the dose-response curves. All experiments were made in triplicate at least three times. Our data were statistically analyzed by one-way ANOVA considering means, SEM, SD, *N*, mean and p value <0.05 not statistically significant.

Docking analysis

The docking complexes of phenyl-amidines (**1a**–**1e**) **1b**, **1c**, **1d**, **1h**, the aryl-amidine **II** and triazolyl-amidines (**2a**, **2b, 2e** and **2f**) with the NMDA receptor and the redocking of ifenprodil were performed using AUTODOCK 4.2 program (32). The 3D structure of the ligands was constructed using SPARTAN'08 as previously described for calculating the stereoeletronic properties. The electrostatic charges were added; the structures were saved in the mol2 format and transferred to AUTODOCK program to create the ligand input file in the pdbqt format. The structure of the N-terminal of GluN1 and GluN2B subunit of NMDA receptor (PDB code = 3QEL) was transferred to AUTODOCK 4.2 program and *Gasteiger* charges were added to create the pdbqt file of the receptor. The cubic grid box with the dimension of 80 × 80 × 80 points and spacing of 0.375 Å was centered in the residue Gln110 of GluN2B subunit and calculated by Autogrid. This residue is located in the ifenprodil binding site and makes hydrogen bond with this ligand in the crystallographic structure.

Docking studies were performed using the empirical free energy function and the Lamarckian genetic algorithm applying a standard protocol, and a total of 50 independent docking runs were carried out for each ligand. Structures differing by less than 2 Å in positional root-mean-square deviation (RMSD) were clustered together and the selected complex for each ligand was that with the lowest binding energy found in the cluster with the greatest number of members.

In silico *ADMET screening*

The four most potent phenyl-amidines and triazolyl-amidines were submitted to an *in silico* ADMET (absorption, distribution, metabolism, excretion, and toxicity) screening, using the Osiris system. The Osiris druglikeness is based on the occurrence frequency of each fragment that is determined within the collection of traded drugs and within the non-drug-like collection of Fluka compounds. The Osiris drug score is related to topological descriptors, fingerprints of molecular druglikeness, structural keys and other properties, such as cLogP and molecular mass.

We also evaluated these compounds according to the Lipinski's modified 'rule-of-five' for successful CNS penetration using the analysis of Osiris program and molinspiration program available at http://www.molinspiration.com/cgi-bin/properties. This rule states molecular mass ≤400 Da, calculated octanol/water partition coefficient (cLogP) ≤5, number of hydrogen bond acceptors (HBA) ≤7, and number of hydrogen bond donors (HBD) ≤3 (33,34).

Results and Discussion

SAR/QSAR analysis of the phenyl-amidine derivatives and design of triazolyl-amidines

In the attempt to provide a useful guideline for the design of more potent GluN1/GluN2B NMDA receptor antagonists, we employed molecular modeling studies to a series of 17 phenyl-amidines described by Claiborne and coworkers (9) as a class of GluN2B-selective NMDA receptor antagonists with the same mechanism of action than ifenprodil. The GluN2B binding data reported utilizes radiolabeled amidine I (KD = 1.0 nM) as the ligand rather than ifenprodil (KD = 94 nM) due to its superior signal-to-noise ratio, and the functional assay (pIC_{50}) was carried out using the FLIPR assay (9). IC_{50} of the most potent compound **1a** was 4.1 nM, and to establish a QSAR analysis, the activities of all phenyl-amidines were described in pIC_{50} here.

The conformational analysis and the MEP maps of the phenyl-amidines (**1a**–**1q**) revealed a similar stereoelectronic 'V' shape with the amidine group in the middle and the phenyl rings in both sides (Figure 2).

The four most potent compounds presented electron-donating groups in R_2 (OMe or Me), which resulted in a negative charge concentrated in the phenyl ring. Meanwhile, most of them presented a less negative charge in

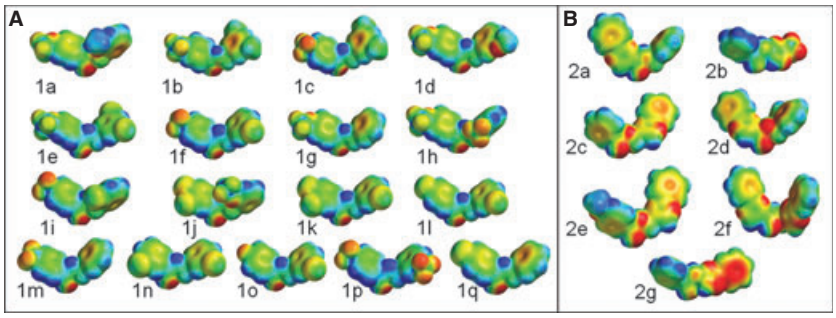

Figure 2: Comparison of molecular electrostatic potential (MEP) maps of the most stable conformation structure of phenyl-amidines (**1a**–**1q**) (A) and triazolyl-amidines (**2a**–**2g**) (B). The negative and positive charge distribution is shown in red and blue, respectively.

R_1 position (i.e., OCF_3, an electron-donating group), or a neutral charge (i.e., CF_3 an electron withdrawing group; Figure 2). Considering the importance of stereoelectronic complementarity for the target receptor interaction, these features probably influenced in the compounds inhibitory profile.

In the SAR/QSAR studies, we calculated some descriptors for these phenyl-amidines (**1a**–**1q**; Table 1). These descriptors were based at least in one of three general characteristics (i.e., electronic, steric, and pharmacokinetic) that could be correlated with the derivative biological profile. Therefore, we calculated electronic (HOMO and LUMO energy and molecular dipole moment), steric (molecular volume, the molecular surface area, and the ovality—a ratio of volume and area), and pharmacokinetic (molecular mass, the octanol/water partition coefficient—cLogP, the water solubility—LogS, and the number of hydrogen bond acceptors—HBA, and donors—HBD) descriptors (Table 1).

Interestingly, our theoretical results revealed important features that could be related to the experimental NMDA receptor antagonist activity. The cross-correlation matrix showed that E_{HOMO}, MV, MSA, ovality, and HBA groups are the most correlated descriptors to the experimental pIC_{50} values (Table 2). It is also possible to observe that the GLUN2B binding assay (pK_i) is directly correlated to the functional assay (pIC_{50}), which reinforced that the antagonistic activity is due to the compounds ability of binding to these receptor subunits.

The structural and electronic properties evaluation showed that HOMO energy of these compounds increased with the biological potency (pIC_{50}), suggesting that the nucleophilicity may be an important feature. The most potent compounds presented higher MV and MSA and, consequently, higher ovality, which are significantly inter-correlated descriptors, that is, $r \geq 0.7$ (Table 2). This means that only one of these descriptors should be selected in a same QSAR equation to avoid model overfitting. The higher number of HBA groups may also be important to interact with the NMDA receptor.

We also performed a multiple linear regression (MLR) analysis to generate a QSAR model for orienting the design of new molecules. On that purpose, we applied the systematic search approach (combining all descriptors in groups of one, two, and three) for variable selection (35), and LOO-CV as an internal validation procedure to examine the correlation of these calculated descriptors with the functional activity (pIC_{50}) of the 17 phenyl-amidines (**1a**–**1q**; Table 1). By analyzing all obtained equations, we have selected eqn 1, as the best model, because it shows the best set of statistical parameters, showing high data fitting ($R = 0.914$). This equation is able to explain 83.6% ($R^2 = 0.836$) of the biological data variance, and present a satisfactory internal predictive ability (LOO-CV R^2 or $Q^2 = 0.609$). Moreover, this model is not overfitted, because it does not contain highly intercorrelated ($r \geq 0.7$) descriptors, as we can see in the cross-correlation matrix (Table 2).

It is interesting to observe that eqn 1 contains one descriptor from each one of the three general characteristics that could explain the structure-activity relationship: electronic (E_{HOMO}), steric (Ovality), and pharmacokinetic (cLogP), where Ovality (steric) has the major contribution, followed by E_{HOMO} (electronic), and finally by cLogP (pharmacokinetic). The potencies predicted by our model (eqn 1) were very similar to those experimentally determined, which could be observed by the maximum (0.59), the minimum (0.02), and the average (0.23) differences between experimental and predicted potencies.

$$pIC_{50} = 2.518 + 0.365(\text{cLogP}) + 1.620(E_{HOMO}) + 12.178(\text{ovality})$$
$$N = 17; R = 0.914; R^2 = 0.836; Q = 0.781; Q^2 = 0.609 \quad (1)$$

Besides the internal validation procedure applied, we also performed an external validation using a test set to confirm the predictive capability of the QSAR model. Four amidines described by Nguyen and co-workers (20) (**3a**, **3b**, **3c** and **3d**) were selected because they present structures similar to the phenyl-amidines used to generate the QSAR model and were tested using the same experimental assay. Our analysis revealed that the pIC_{50} predicted for the compounds **3a**–**3d** were very similar to the experimental pIC_{50}. Only in case of **3b,** the difference between the experimental and the predicted potency was higher than those observed in the phenyl-amidine series; however, it may be considered an outlier. The *Ki* described in the literature (20) for **3b** was the highest among this group, and as the pK_i was directly correlated with the pIC_{50} in the phenyl-amidines series, we expected higher experimental pIC_{50} for **3b**. Also, comparing with the phenyl-amidines, **3b** present the same substituents (4-OCF_3 and 3,5 diMe) than **1b** that was described with higher activity (Table 3). Thus, the equation was able to predict the activity of this series (**3a**–**3d**) and was also used to predict the activity of the triazolyl-amidines.

Two new triazolyl-amidine derivatives (**2a** and **2b**) were designed in this study by combining the amidine group, that has already been tested as NMDA receptor antagonist (9) and triazolyl groups-1,2,3-triazole (**2a**) and 1,2,4-triazole (**2b**; Figure 1). Historically, two key features in the early GluN2B antagonists were phenols and basic amines. Within this series of compounds, the phenol can be problematic in metabolic clearance, whereas the basic amine can give rise to hERG and other issues such as potent CYP2D6 inhibition. The structures of **2a** and **2b** were designed by ligand-based drug design using molecular modification strategies as bioisosterism and SAR. The pharmacophore of the NMDA receptor non-competitive antagonists were conserved as: one aromatic group in

Table 1: Comparison of the experimental biological data (pK_i and pIC_{50}) of the 17 phenyl-amidine compounds (**1a**–**1q**) from the literature (9) with the calculated descriptors: E_{HOMO} and E_{LUMO} (HOMO and LUMO Energies, Ev), μ (Molecular Dipole Moment, Debye), MV (Molecular Volume, Å^3), MSA (Molecular Surface Area, Å^2), Ovality (a ratio of volume and area), MM (Molecular Mass, g/mol), cLogP (calculated octanol/water partition coefficient), cLogS (calculated water solubility), and HBA (number of hydrogen bond acceptors, i.e., N and O atoms)

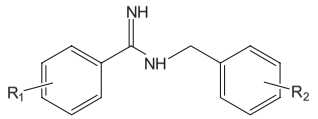

Compounds no.	R_1	R_2	pK_i	pIC_{50}[a]	pIC_{50}Calc[b]	pIC_{50}[a] – pIC_{50}Calc[b]	E_{HOMO}	E_{LUMO}	μ	MV	MSA	Ovality	MM	cLogP	LogS	HBA[c]
1a	4-OCF3	2-OMe	7.24	8.39	8.09	0.30	–8.65	2.98	3.57	307.64	334.85	1.52	324.30	2.97	–3.16	4
1b	4-OCF3	3,5diMe	7.80	8.38	8.29	0.09	–8.80	2.79	1.95	313.44	342.25	1.53	322.33	3.71	–3.84	3
1c	4-CF3	3,5-diMe	7.41	8.06	8.23	–0.17	–8.79	2.14	2.77	308.22	337.52	1.53	306.33	3.64	–3.59	2
1d	4-OCF3	3-OMe	6.64	8.01	8.33	–0.32	–8.56	2.87	2.73	307.85	336.89	1.53	324.30	2.97	–3.16	4
1e	4-OCF3	3,5diCl	8.22	7.62	7.49	0.13	–9.41	2.70	1.23	307.06	337.12	1.53	363.16	4.30	–4.62	3
1f	4-CF3	3-Cl	6.70	7.49	7.11	0.38	–9.21	2.04	1.19	285.16	313.07	1.49	312.72	3.62	–3.64	2
1g	4-OCF3	H	5.92	7.34	6.95	0.39	–9.09	2.85	1.52	280.49	307.02	1.48	294.27	3.08	–3.15	3
1h	4-OCF3	2-CF3	6.49	7.33	7.26	0.07	–9.36	2.57	3.77	312.60	338.33	1.52	362.17	3.84	–3.92	3
1i	4-CF3	2-Cl	6.25	7.32	6.73	0.59	–9.36	2.15	2.48	284.89	310.37	1.48	312.72	3.62	–3.64	2
1j	3,4diCl	2-OCF3	7.14	7.24	7.40	–0.16	–9.30	2.52	4.11	306.55	331.73	1.51	363.16	4.30	–4.62	3
1k	3,4diCl	3-Cl	7.89	6.96	7.16	–0.20	–9.18	2.40	2.48	278.74	305.34	1.48	313.61	4.09	–4.33	2
1l	4-Cl	3-Cl	6.20	6.80	6.76	0.04	–9.12	2.69	1.90	265.58	291.04	1.46	279.17	3.47	–3.60	2
1m	4CF3	H	5.32	6.44	6.64	–0.20	–9.17	2.13	2.46	271.86	297.95	1.47	278.27	3.01	–2.90	2
1n	3-Cl	3-Cl	5.10	6.38	6.76	–0.38	–9.12	2.74	3.57	265.58	291.04	1.46	279.17	3.47	–3.60	2
1o	4-F	3-Cl	5.22	6.35	6.37	–0.02	–9.12	2.95	1.82	257.18	281.97	1.44	262.71	2.92	–3.17	2
1p	4-CF3	3-CF3	5.15	6.18	6.54	–0.36	–9.87	1.96	2.60	304.72	335.07	1.53	346.27	3.77	–3.68	2
1q	4-Cl	H	5.01	6.14	6.29	–0.15	–9.06	2.77	1.65	252.28	275.92	1.43	244.72	2.86	–2.86	2

[a]Experimental values of pK_i (*M*) and pIC_{50} (*M*) were described in the literature (9).
[b]The pIC_{50} values were calculated using eqn 1.
[c]Number of hydrogen bond donors (HBD, i.e., NH and OH groups) = 2 for all compounds.

Table 2: Cross-correlation matrix of the experimental biological activities (pK_i and pIC_{50}) for the 17 phenyl-amidine compounds (**1a**–**1q**) from the literature (9) and the calculated descriptors: E_{HOMO} and E_{LUMO} (HOMO and LUMO Energies, Ev), μ (Molecular Dipole Moment, Debye), MV (Molecular Volume, Å^3), MSA (Molecular Surface Area, Å^2), Ovality (a ratio of volume and area), MM (Molecular Mass, g/mol), cLogP (calculated octanol/water partition coefficient), cLogS (calculated water solubility), and HBA (number of hydrogen bond acceptors, i.e., number of N and O atoms)

	pIC_{50}	pK_i	E_{HOMO}	E_{LUMO}	μ	MV	MSA	Ovality	MM	cLogP	cLogS	HBA
pIC_{50}	1.00											
pK_i	0.78	1.00										
E_{HOMO}	0.60	0.27	1.00									
E_{LUMO}	0.19	0.05	0.54	1.00								
μ	0.09	0.01	0.06	0.02	1.00							
MV	0.74	0.65	0.08	−0.12	0.36	1.00						
MSA	0.74	0.66	0.07	−0.13	0.32	1.00	1.00					
Ovality	0.72	0.65	0.05	−0.18	0.25	0.98	0.99	1.00				
MM	0.48	0.61	−0.29	−0.19	0.37	0.88	0.87	0.85	1.00			
cLogP	0.15	0.60	−0.50	−0.37	0.17	0.48	0.48	0.48	0.73	1.00		
cLogS	−0.20	−0.66	0.40	0.17	−0.18	−0.46	−0.46	−0.45	−0.72	−0.97	1.00	
HBA	0.69	0.43	0.49	0.57	0.30	0.63	0.61	0.57	0.50	−0.08	−0.04	1.00

Table 3: Comparison of the experimental biological data (pIC_{50}) described in the literature (20) and the predicted pIC_{50} (*M*) of four amidines used as test set. The theoretical descriptors used to calculate pIC_{50} – E_{HOMO} (HOMO Energy Ev), Ovality (a ratio of volume and area) and the cLogP (calculated octanol/water partition coefficient)—were described

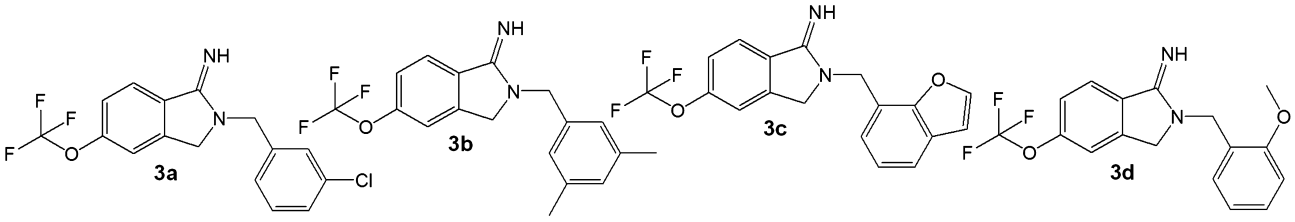

Compounds no.	cLogP	E_{HOMO}	Ovality	pIC50[a]	$pIC_{50}Calc$[b]	pIC_{50} – pIC_{50Calc}
3a	3.25	−9.08	1.49	7.31	7.14	0.17
3b	3.27	−8.72	1.52	7.41	8.10	−0.69
3c	3.03	−8.41	1.49	7.92	8.14	−0.22
3d	2.53	−8.60	1.50	8.22	7.78	0.44

[a]Experimental values of pIC_{50} (*M*) were described in the literature (20).
[b]The predicted pIC_{50} values were calculated using eqn 1.

each side connected by an aliphatic chain with a hydrogen bond donor group. In this study we evaluated the addition of the triazole ring that is an important moiety in many bioactive compounds. In each molecule (**2a** and **2b**), this group was added in one and in the other side of the amidine group to test the effect. Also, the group CF_3 present in some phenyl-amidines was tested in **2b** (Figure 1).

Initially, the comparison of the same descriptors calculated for the phenyl-amidine derivatives showed compound **2a** with high number of HBA groups and HOMO energy value similar to the most potent phenyl-amidines, while **2b** presented only higher number of HBA groups than the most potent phenyl-amidines (Tables 1 and 4).

The analysis of the electrostatic potential maps and the structure of the best conformer of the triazolyl-amidines (**2a** and **2b**) revealed a stereoelectronic 'V' shape similar to that observed for phenyl-amidines (**1a**–**1q**). The electronic property analysis revealed electron density in the phenyl ring of **2a**. In case of **2b** that do not present the phenyl group at this position, the negative charge is related to the CF_3 group (Figure 2). The QSAR model applied to the designed triazolyl-amidines showed a higher activity for compound **2a** compared with **2b**.

Synthesis of new triazolyl-amidines

To evaluate the neuroprotective profile of the triazolyl-amidines derivatives against glutamate side-effects, we synthetized compounds **2a** and **2b**, rationally designed in this work. The reaction of the aldehyde **3** (36) with hydroxylamine cloridrate generated the 1,2,3-triazole oxime **4** (37), which on treatment with acetic anhydride led to the

Table 4: Comparison of the theoretical descriptors of the QSAR-based designed triazolyl-amidines (**2a**–**2g**). The analysis included the predicted pIC_{50} (*M*) and the calculated descriptors E_{HOMO} (HOMO Energy Ev) MV (Molecular Volume Å3) MSA (Molecular Surface Area Å2) Ovality (a ratio of volume and area) and the pharmacokinetic properties for a good oral for CSN drugs bioavailability that include MM (Molecular Mass g/mol) cLogP (calculated octanol/water partition coefficient) HBA (number of hydrogen bond acceptors) HBD (number of hydrogen bond donors) PSA (polar surface area) and RotB (number of rotatable bonds)

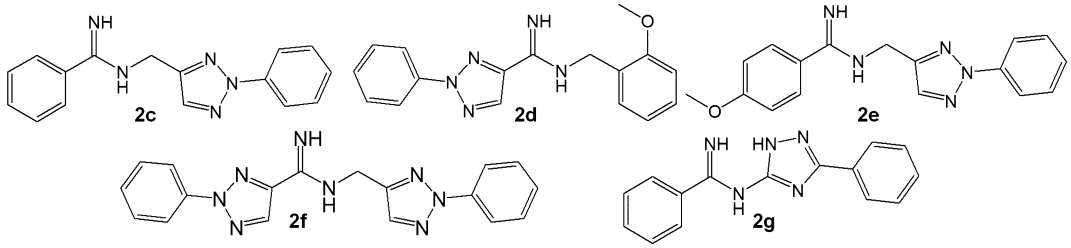

						Pharmacokinetic properties					
Compounds no.	pIC_{50Pred}[a]	E_{HOMO}	MV	MSA	Ovality	MM	cLogP	HBA	HBD	PSA	RotB
2a	7.65	–8.72	293.42	319.02	1.49	277.33	3.05	5	2	50.50	4
2b	4.97	–9.47	221.81	251.72	1.42	255.20	1.38	5	3	62.72	2
2c	7.92	–8.63	293.68	320.20	1.50	277.33	3.05	5	2	52.18	3
2d	8.28	–8.61	321.02	350.03	1.53	307.36	2.95	5	2	56.63	5
2e	8.37	–8.63	320.71	347.34	1.54	307.33	2.95	5	2	59.34	5
2f	9.34	–8.54	348.40	379.27	1.58	344.38	3.86	8	2	74.42	4
2g	8.37	–7.91	272.88	295.98	1.46	263.30	2.42	5	3	62.47	2

[a]The predicted pIC_{50} values were calculated using eqn 1.

corresponding 1,2,3-triazole nitrile **5** (38). In a modified procedure, carried out in DMSO as the solvent, the reaction of **5** with benzylamine in cuprous chloride at 80 °C (39) produced the novel 1,2,3-triazole amidine **2a** in good yield (73%; Figure 3).

The reaction of trifluoroacetic acid with aminoguanidine bicarbonate led to the 1,2,4-triazole **6** as described in the literature (40). The subsequent treatment of **6** with benzonitrile in the presence of cuprous chloride at 80 °C produced, regioselectively, the novel 1,2,4-triazole amidine **2b** in good yield (75%; Figure 3) (39).

Neuroprotection from glutamate excitotoxicity

Previous work showed that the excitotoxicity induced by glutamate in avian retinal neurons cultures is directly related to the agonist glutamate binding to NMDA receptors because this excitotoxicity is completely blocked by the NMDA channel blocker MK-801 (28). To test the ability of the triazolyl-amidines to protect neuronal cells from glutamate excitotoxicity, we pre-incubated these neurons cultures with the triazolyl-amidines (**2a** and **2b**; 100 nM) before the addition of glutamate (1 mM) as described in materials and methods section (Figure 4).

Our assays confirmed that glutamate promotes an extensive cell death (77% of total cells) after incubation for 8 h compared with control without glutamate. Interestingly, both compounds **2a** and **2b** protected the neurons from the glutamate effect (from 77% to 27% and 45%, respectively), values close to that detected for Ifenprodil, in this assay and in the literature (Figure 4) (29,30). No significant effect was observed when incubating these compounds with the neuron cultures without adding glutamate suggesting a safe profile. Our results suggest a better profile

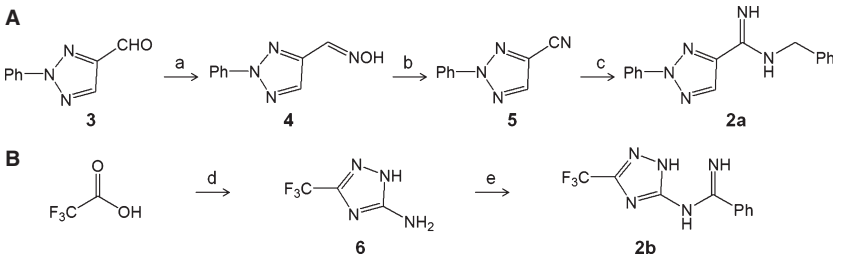

Figure 3: (A) Synthesis route of triazolil-amidines **2a**. (a) $NH_2OH.HCl$, $NaHCO_3$, Na_2SO_4, CH_2Cl_2, r.t., 18 h, 87%. (b) Ac_2O, reflux, 2 h, 70%. (c) $BnNH_2$, CuCl, DMSO, 80 °C, 20 h, 73%. (B) Synthesis route of triazolil-amidine **2b**. (d) aminoguanidine bicarbonate, toluene, reflux, 20 h, 91%. (e) PhCN, CuCl, 80 °C, 20 h, 75%.

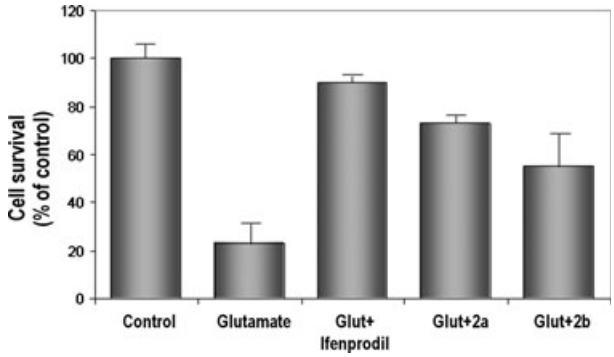

Figure 4: Neuroprotective effect of pre-incubation (48 h) of triazolyl-amidines **2a** and **2b** and the reference compound ifenprodil from glutamate-induced excitotoxicity.

for **2a**, but anyway both **2a** and **2b** presented some neuroprotective activity, which points to the promising profile of the triazolyl-amidine series.

Cytotoxicity assays

In this study, we evaluated the cytotoxicity profile using different concentrations of the triazolyl-amidines on Vero cells (Figure 5). Our experimental results showed that both molecules **2a** and **2b** present a safe profile with a CC_{50} (1402.00 and 1403.51 μM, respectively). The low cytotoxic profile of these compounds reinforced the theoretical results predicted herein that suggested that they might present a safe profile as therapeutic agents.

Design of the triazolyl-amidines and docking evaluation

To improve the overall potential of these two compounds as neuroprotective molecules, we suggested some structural modifications based on the phenyl-amidines analysis

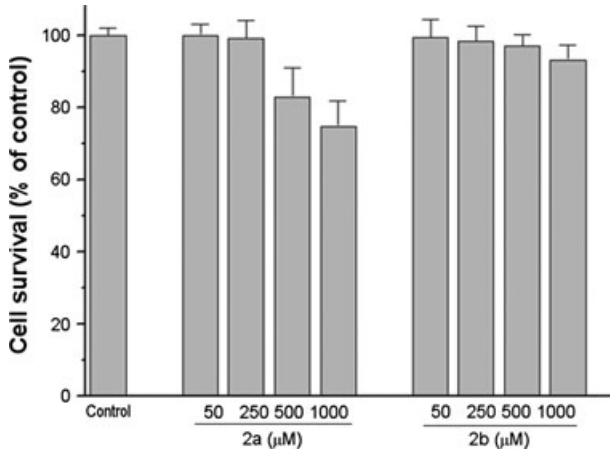

Figure 5: Cytotoxicity profile (Vero cells) of triazolyl-amidines **2a** and **2b** in the concentration of 50, 250, 500, and 1000 μM. The data represent the mean ± SEM from three individual experiments.

generating the compounds **2c**–**2g** (Table 4). Thus, we used the triazolyl group in each side of the molecule and in both sides simultaneously (**2f**) also adding some substitutions based on the most potent phenyl-amidines. The analysis of the descriptors initially calculated for the phenyl-amidine derivatives, showed that our rational design allowed to increase values of HOMO energy, MV (volume), and MSA (area), and to preserve the number of HBA groups for all new compounds, except for **2f**. Importantly, the HOMO energy values (–8.63 to –7.91 eV) of these compounds were similar to that observed for the four most potent phenyl-amidines (–8.80 to –8.56 eV) as well as MV (272.88–348.40 $Å^3$ and 307.64–313.44 $Å^3$), MSA (295.27–379.98 $Å^2$ and 334.85–342.25 $Å^2$), and ovality (1.46–1.58 and 1.52–1.53), respectively (Tables 1 and 3).

To predict the biological potency (pIC_{50Pred}) of compounds **2a**–**2g,** we applied the QSAR eqn 1 derived from 17 phenyl-amidines (**1a**–**1q**). According to our model, except for compound **2b** (pIC_{50Pred} = 4.97 *M*), the calculated potencies for the other triazolyl-amidines were similar to or better than the most potent phenyl-amidines (**1a**–**1d**; Tables 1 and 4).

The analysis of the electrostatic potential maps and the structure of the best conformer of the triazolyl-amidines (**2c**–**2g**) also reinforced the data revealing a stereoelectronic 'V' shape with similar charge distribution than that observed for phenyl-amidines (**1a**–**1q**; Figure 2).

Recently, Karakas and co-workers (41) elucidated the structure of the N-terminal of GluN1 and GluN2B subunit of NMDA receptor from *Rattus norvegicus* (PDB code = 3-QEL) complexed with ifenprodil. The protein structure was used to perform the docking with the amidines studied here and theoretically analyze and compare their binding mode. Initially, the ifenprodil was redocked in the binding site to validate the method. Our results showed the ifenprodil interacting in almost the same position than in the crystallographic structure (RMSD = 0.95 Å).

We evaluated the interactions of some phenyl-amidines (**1b, 1c, 1d** and **1h**), the aryl-amidine II, the synthesized triazolyl-amidines **2a** and **2b**, and the designed **2e** and **2f** with the receptor to complement and support the QSAR study and propose a mechanism of action for the triazolyl-amidines. The conformation/position chosen was the one with lower energy in the most populated cluster. The comparison of the dockings of triazolyl-amidines **2a, 2b, 2e,** and **2f** with the NMDA receptor revealed that one of the phenyl rings in all triazolyl-amidines was aligned and that the triazolyl ring in **2a, 2e** and **2f** was also aligned. In case of **2b,** although the triazolyl is not aligned, it presents nitrogen atoms in positions similar to the other derivatives. The other phenyl ring of **2a**, **2e** and **2f** was also in similar region. The conformation and binding mode in the active site of NMDA receptor is similar for these triazolyl-amidines and the amidines **II** and **1b** (Figure 6).

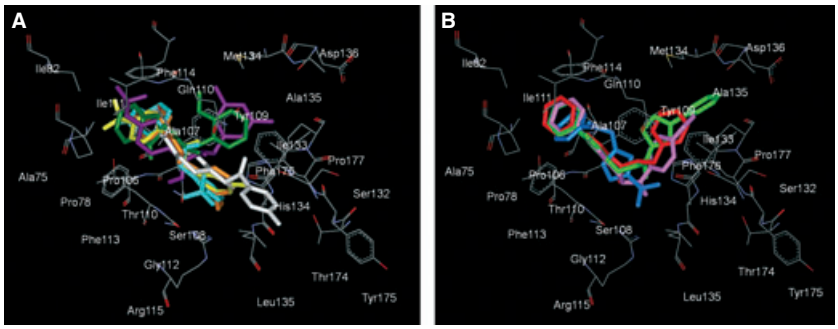

Figure 6: Comparison of the binding mode of the NMDA receptor antagonists described in the literature (A) and the designed triazolyl-amidines (B). Ligands are represented in different colors: **II** (dark green), **1b** (purple), **1c** (yellow), **1d** (orange), **1h** (light blue), ifenprodil (white), **2a** (red), **2b** (blue), **2e** (pink) and **2f** (light green).

Ifenprodil and the phenyl-amidines also conserved one of the phenyl rings in a similar position than the triazolyl-amidines, while the position of the other phenyl ring of **1c**, **1d, 1h,** and ifenprodil are slight different. Although this, nitrogen atoms of the amidines are in similar positions than the nitrogen of the piperidine of ifenprodil (Figure 6).

In all triazolyl-amidines, the residues Y109, T110, F113, S132 and I133 of GluN1 and A107, Q110 and I111 of GluN2B were described interacting at 4 Å distant from the receptor; these residues were also interacting in phenyl-amidines. Hydrogen bonds with the residues Y109 of GluN1 and Q110 of GluN2B were observed in all triazolyl-amidines, and some of them also interacted with F113, I133 and L135 of GluN1 and A107 and I111 of GluN2B. The phenyl-amidines and ifenprodil also interacted with some of these residues (Y109, F113, I133, L135, Q110 and A107), but some interactions with the GluN1 subunit were different (S108 and S132; Table 5).

Hydrophobic interactions with the residue L135 was observed in phenyl-amidines **1c**, **1d**, **1h** and ifenprodil, while triazolyl-amidines and the amidines **II** and **1b** interacted with I133 and M134. This data reveal that although the triazolyl-amidines present similar binding mode in the ifenprodil binding site than some phenyl-amidines, which justifies the SAR done, they may test different residues of the active site, and it may be important for future modifications in this series to improve the biological activity.

Table 5: Residues of GluN1/GluN2B subunit of NMDA receptor involved in the interactions with the ifenprodil, phenyl-amidine **1b, 1c, 1d, 1h**, aryl-amidine **II** and triazolyl-amidines **2a**, **2e,** and **2f** and residues interacting with the ligands by hydrogen bonds

Compounds no.	Residues of GluN1 interacting with the ligand (4 Å)	Residues of GluN2B interacting with the ligand (4 Å)	Hydrogen bonds in GluN1	Hydrogen bonds in GluN2B
Ifenprodil	Y109, T110, R115, S132, I133, L135	A107, Q110, I111, F114, T174, Y175, F176, P177, E236	S132	Q110
II	A75, Y109, T110, F113, S132, I133	P78, I82, A107, Q110, I111, F114, M134	Y109	Q110, A107
1b	Y109, G112, F113, S132, I133	P78, I82, Q110, I111, F114, M134, P177	Y109, F113	Q110
1c	A75, P106, S108, Y109, T110, G112, F113, S132, I133, H134, L135	P78, I82, A107, Q110, I111, F114	–	Q110, A107
1d	A75, P106, S108, Y109, T110, G112, F113, S132, I133, H134, L135	A107, Q110, I111, F114	S108, I133, L135	Q110, A107
1h	A75, P106, S108, Y109, T110, G112, F113, R115, I133, L135	I82, A107 Q110, I111, F114	–	Q110, A107
2a	Y109, T110, G112, F113, S132, I133	P78, I82, A107, Q110, I111, F114, M134, P177	Y109, F113	Q110
2b	S108, Y109, T110, G112, F113, S132, I133, L135	P78, A107, Q110, I111	Y109, F113	Q110, I111, A107
2e	S108, Y109, T110, G112, F113, S132, I133, L135	P78, A107, Q110, I111, F114, P177	Y109, F113, I133, L135	Q110
2f	Y109, T110, F113, S132, I133	P78, I82, A107, Q110, I111, F114, M134, A135, D136, P177	I133	Q110

In silico *ADMET screening*

To analyze the overall theoretical potential of the triazolyl-amidine series as drug candidates and to compare with the four most potent amidines, we submitted the triazolyl-amidines (**2a**–**2g**) to an *in silico* ADMET screening using the Osiris system.

According to the Osiris property evaluation, the lipophilicity (cLogP) of these triazolyl-amidines (**2a**–**2g**; 1.38–3.86) was similar to that observed for the most potent phenyl-amidines (**1a**–**1d**; 2.97–3.71) and pointed the compounds as sufficiently hydrophobic for penetrating the biological membranes (Tables 1 and 3). We noticed that the triazolyl-amidines presented a better profile of druglikeness and drug score than phenyl-amidines and druglikeness values lower than ifenprodil and Co101676 and CI1041, other NMDA receptor antagonists (Figure 7).

Literature described that CNS drugs that penetrate blood–brain barrier are more lipophilic, less polar, less flexible, and with lower molecular mass and volume than other classes of drugs. Because the compounds are considered for oral delivery and should be able to cross the blood–brain barrier into the CNS, they were evaluated according to the Lipinski modified 'rule-of-five' for successful CNS penetration. Interestingly, our theoretical results showed all triazolyl-amines and the four most potent phenyl-amidines compounds as fulfilling the Lipinski modified 'rule-of-five' for successful CNS penetration, with MM ≤400 Da, cLogP ≤5, number of HBA ≤7, and number of HBD ≤3. In fact, the rule states that at least three of these requirements should be satisfied for a drug good bioavailability.

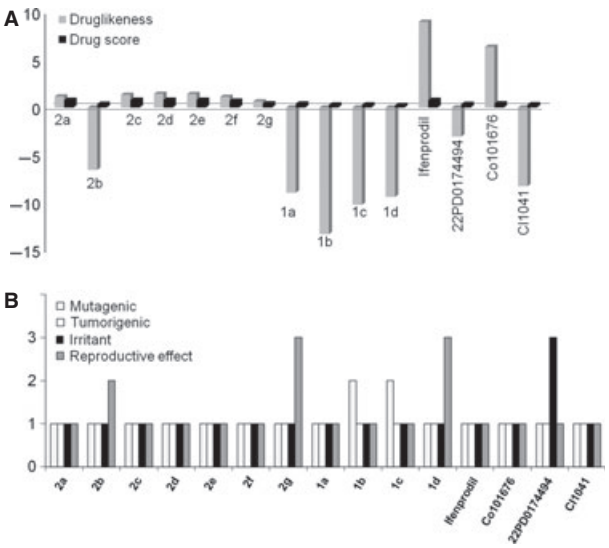

Figure 7: Comparison of Druglikeness and Drug score Profiles (A) and toxicity risks (B) of the most potent phenyl-amidines (**1a**–**1d**) the triazolyl-amidines (**2a**–**2g**) and some NMDA receptor antagonists (ifenprodil, Co101676, PD0174494, and CI-1041 calculated using Osiris Property Explorer.

Interestingly, CNS drugs should have polar surface area (PSA) <60–70Å^2 and number of rotatable bonds (RotB) <8 such as observed for all triazolyl-amidines, except for **2f** (74.42Å), that is still lower than the upper limit for penetrate the brain (~90Å^2; Table 4).

The Osiris toxicity evaluation showed most of the triazolyl-amidines with a low profile for irritant, tumorigenic, mutagenic, and reproductive effects, except for **2b** and **2g** (1,2,4-triazolyl-amidines) that presented some teratogenic risks analogously to **1d**. The NMDA receptor antagonist PD1724494 showed a high irritant risk, while the phenyl-amidines **1b** and **1c** presented mutagenic risks (Figure 7). It is important to notice that the toxicity predicted herein does not guarantee that these compounds are completely free of any toxic effect. However, it reinforced the promising potential of this series.

Conclusions

The overall SAR analysis of 17 phenyl-amidines (**1a**–**1q**) described in the literature revealed structural descriptors and electronic properties that could be related to the biological profile. Higher values of HOMO energy, molecular volume, molecular surface area, ovality, and number of hydrogen bond acceptor groups were apparently the most correlated descriptors with the interaction with NMDA receptor. The results of molecular modeling techniques applied on the phenyl-amidine series enabled the design of new triazolyl-amidines (**2a** and **2b**) with neuroprotective activity against glutamate side-effects besides low toxicity. With the promising profile of this new triazolyl-amidines series, in the future, other substitutents may be tested to improve the biological activity of **2a** and **2b**. These data may lead to more effective and less toxic compounds for treating neurodegenerative disorders involving NMDA receptors.

Acknowledgments

Research fellowships from Brazilian agencies granted to H.C.C. (FAPERJ), R.P.C (CNPq), I.C.P.P.F. (CNPq), P.A.A. (CNPq), V.A.G.G.S. (FIOTEC), J.M.F. (CAPES), O.M.C. (CNPq), R.A.C.L. (FAPERJ), L.M.S.M. (CAPES), and A.M.H. (CNPq) are gratefully acknowledged. This work was partially supported by CAPES, CNPq, FAPERJ, FIOTEC, Instituto de Biologia/UFF, Instituto de Química/UFF, Faculdade de Farmácia/UFRJ, Instituto de Química/UFRJ (CNPq/PIBIC) and NPPN/UFRJ.

Conflict of Interest

All authors declare that there are no financial and/or commercial conflicts of interest.

References

1. Marinelli L., Cosconati S., Steinbrecher T., Limongelli V., Bertamino A., Novellino E., Case A.D. (2007) Homology modeling of NR2B modulatory domain of NMDA receptor and analysis of ifenprodil binding. Chem Med Chem;2:1498–1510.
2. Traynelis S.F., Wollmuth L.P., McBain C.J., Menniti F.S., Vance K.M., Ogden K.K., Hansen K.B., Yuan H., Myers S.J., Dingledine R. (2010) Glutamate receptor ion channels: structure, regulation, and function. Pharmacol Rev;62:405–496.
3. Furukawa H., Singh S.K., Mancusso R., Gouaux E. (2005) Subunit arrangement and function in NMDA receptors. Nature;438:185–192.
4. Nikam S.S., Meltzer L.T. (2002) NR2B selective NMDA receptor antagonists. Curr Pharm Des;8:845–855.
5. Armstrong N., Gouaux E. (2000) Mechanisms for activation and antagonism of an AMPA-sensitive glutamate receptor: crystal structures of the GluR2 ligand binding core. Neuron;28:165–181.
6. Barta-Szalai G., Borza I., Bozo E., Kiss C., Ágai B., Proszenyák A., Keseru G.M., Gere A., Kolok S., Galgóczy K., Horváth C., Farkas S., Domány G. (2004) Oxamides as novel NR2B selective NMDA receptor antagonists. Bioorg Med Chem Lett;14:3953–3956.
7. Gogas K.R. (2006) Glutamate-based therapeutic approaches: NR2B receptor antagonists. Curr Opin Pharmacol;6:68–74.
8. Brown D.G., Maier D.L., Sylvester M.A., Hoeter T.N., Menhaji-Klotz E., Lasota C.C., Hirata L.T. *et al.* (2011) 2, 6-Disubstituted pyrazines and related analogs as NR2B site antagonists of the NMDA receptor with antidepressant activity. Bioorg Med Chem Lett;21:3399–3403.
9. Claiborne C.F., McCauley J.A., Libby B.E., Curtis N.R., Diggle H.J., Kulagowski J.J., Michelson S.R., *et al.* (2003) Orally efficacious NR2B-selective NMDA receptor antagonists. Bioorg Med Chem Lett;13:697–700.
10. Max M.B., Byas-Smith M.G., Gracely R.H., Bennett G.J. (1995) Intravenous nfusion of the NMDA antagonist, ketamine, in chronic posttraumatic pain with allodynia: a double-blind comparison to alfentanil and placebo. Clin Neuropharmacol;18:360–368.
11. Muir K.W., Lees K.R. (1995) Clinical experience with excitatory amino acid antagonist drugs. Stroke;26:503–513.
12. Tikhonova I.G., Baskin I.I., Palyulin V.A., Zefirov N.S., Bachurin S.O. (2002) Structural basis for understanding structure-activity relationships for the glutamate binding site of the NMDA receptor. J Med Chem;45:3836–3843.
13. Curtis N.R., Diggle H.J., Kulagowski J.J., London C., Grimwood S., Hutson P.H., Murray F., Richards P., Macaulay A., Wafford K.A. (2003) Novel N1-(benzyl)cinnamamidine derived NR2B subtype-selective NMDA receptor antagonists. Bioorg Med Chem Lett;13:693–696.
14. Ogden K.K., Traynelis S.F. (2011) New advances in NMDA receptor pharmacology. Trends Pharmacol Sci;32:726–733.
15. Chenard B.L., Menniti F.S. (1999) Antagonists selective for NMDA receptors containing the NR2B subunit. Curr Pharm Des;5:381–404.
16. McCauley J.A., Theberge C.R., Romano J.J., Billings S.B., Anderson K.D., Claremon D.A., Freidinger R.M. *et al.* (2004) NR2B-selective N-methyl-D-aspartate antagonists: synthesis and evaluation of 5-substituted benzimidazoles. J Med Chem;47:2089–2096.
17. Borza I., Domany G. (2006) NR2B selective NMDA antagonists: the evolution of the ifenprodil-type pharmacophore. Curr Top Med Chem;6:687–695.
18. Layton M.E., Kelly M.J. III, Rodzinak K.J. (2006) Recent advances in the development of NR2B subtype-selective NMDA receptor antagonists. Curr Top Med Chem;6:697–709.
19. Borza I., Kolok S., Ignacz-Szendrei G., Greiner I., Tarkanyi G., Galgoczy K., Horvath C., Farkas S., Domany G. (2005) Indole-2-carboxamidines as novel NR2B selective NMDA receptor antagonists. Bioorg Med Chem Lett;15:5439–5441.
20. Nguyen K.T., Claiborne C.F., McCauley J.A., Libby B.E., Claremon D.A., Bednar R.A., Mosser S.D., Gaul S.L., Connoly T.M., Condra C.L., Bednar B., Stump G.L., Lynch J.J., Koblan K.S., Liverton N.J. (2007) Cyclic benzamidines as orally efficacious NR2B-selective NMDA receptor antagonists. Bioorg Med Chem Lett;17:3997–4000.
21. De La Rosa M., Kim H.W., Gunic E., Jenket C., Boyle U., Koh Y., Korboukh I. *et al.* (2006) Tri-substituted triazoles as potent non-nucleoside inhibitors of the HIV-1 reverse transcriptase. Bioorg Med Chem Lett;16:4444–4449.
22. Witkowski J.T., Robins R.K., Khare G.P., Sidwell R.W. (1973) Synthesis and antiviral activity of 1,2,4-triazole-3-thiocarboxamide and 1,2,4-triazole-3-carboxamidine ribonucleosides. J Med Chem;16:935–937.
23. Costa M.S., Boechat N., Rangel E.A., da Silva F.C., de Souza A.M., Rodrigues C.R., Castro H.C., Júnior I.N., Lourenço M.C.S., Wardell S.M.S.V., Ferreira V.F. (2006) Synthesis, tuberculosis inhibitory activity, and SAR study of N-substituted-phenyl-1,2,3-triazole derivatives. Bioorg Med Chem;14:8644–8653.
24. Cunha A.C., Figueiredo J.M., Tributino J.L., Miranda A.L., Castro H.C., Zingali R.B., Fraga C.A.M., de Souza M.C.B.V., Ferreira V.F., Barreiro E.J. (2003) Antiplatelet properties of novel N-substituted-phenyl-1,2,3-triazole-4-acylhydrazone derivatives. Bioorg Med Chem;11:2051–2059.
25. Kelley J.L., Koble C.S., Davis R.G., McLean E.W., Soroko F.E., Cooper B.R. (1995) 1-(Fluorobenzyl)-4-amino-1H-1,2,3-triazolo(4,5-c)pyridines: synthesis and anticonvulsant activity. J Med Chem;38:4131–4134.
26. Biagi G., Dell'Omodarme G., Ferretti M., Giorgi I., Livi O., Scartoni V. (1992) Structure-activity studies on a

1,2,3-triazole derivative, a potent in vitro inhibitor of prostaglandin synthesis: the role of the heterocyclic ring. Farmaco;47:335–344.
27. Sander T. (2001) OSIRIS Property Explorer. Organic Chemistry Portal. Available at: http://www.organic-chemistry.org/prog/peo/.
28. Ferreira J.M., Paes-de-Carvalho R. (2001) Long-term activation of adenosine A2a receptors blocks glutamate excitotoxicity in cultures of avian retinal neurons. Brain Res;900:169–176.
29. Zhang S., Kashii S., Yasuyoshi H., Kikuchi M., Honda Y., Kaneda K., Sato S., Akaike A. (2000) Protective effects of ifenprodil against glutamate-induced neurotoxicity in cultured retinal neurons. Graefes Arch Clin Exp Ophthalmol;238:846–852.
30. Adler R., Lindsey J.D., Elsner C.L. (1984) Expression of cone-like properties by chick embryo neural retina cells in glial-free monolayer cultures. J Cell Biol;99:1173–1178.
31. Mosmann T. (1983) Rapid colorimetric assay for cellular growth and survival: application to proliferation and cytotoxicity assays. J Immunol Methods;65:55–63.
32. Goodsell D.S., Morris G.M., Olson A.J. (1996) Automated docking of flexible ligands: applications of AutoDock. J Mol Recognit;9:1–5.
33. Lipinski C.A., Lombardo F., Dominy B.W., Feeney P.J. (2001) Experimental and computational approaches to estimate solubility and permeability in drug discovery and development settings. Adv Drug Deliv Rev;46:3–26.
34. Pajouhesh H., Lenz G.R. (2005) Medicinal chemical properties of successful central nervous system drugs. NeuroRx;2:541–553.
35. Ferreira M.M.C., Montanari C.A., Gaudio A.C. (2002) Seleção de variáveis em QSAR. Quím Nova;25:439–448.
36. da Silva R.C. Jr, Ferreira V.F., Pinheiro S. (2004) The stereoselective synthesis of nopinone based triazole ketones. Tetrahedron-Asymmetr;15:3719–3722.
37. El Khadem H., El-Shafei Z., Meshreki M., Shaban M. (1966) Derivatives of osotriazoles and 4-formyl-2-phenyl-1, 2, 3-triazole. J Chem Soc C;0:91–93.
38. Begtrup M., Holm J. (1981) Electrophilic and nucleophilic substitution in the triazole N-oxides and N-methoxytriazolium salts: preparation of substituted 1, 2, 3-triazoles. J Chem Soc Perkin Trans;1:503–513.
39. Rousselet G., Capdevielle P., Maumy M. (1993) Copper (I)-induced addition of amines to unactivated nitriles: the first general one-step synthesis of alkyl amidines. Tetrahedron Lett;34:6395–6398.
40. Zohdi H.F. (1997) Reactions with 3-amino-5-trifluoromethyl-1,2,4-triazole: a simple route to fluorinated polysubstituted triazolo (1, 5-a) pyrimidine and triazolo (5, 1-c) triazine derivatives. J Chem Res-S;5:392–393.
41. Karakas E., Simorowski N., Furukawa H. (2011) Subunit arrangement and phenylethanolamine binding in GluN1/GluN2B NMDA receptors. Nature;475:249–253.